Magnetic phase diagram of $CuGe_{1-x}Si_xO_3$

M. Weiden, R. Hauptmann, W. Richter, C. Geibel, P. Hellmann, M. Köppen, and F. Steglich
FG Technische Physik, TH Darmstadt, Hochschulstraße 8, 64289 Darmstadt, Germany

M. Fischer, P. Lemmens, and G. Güntherodt
2. Physikalisches Institut, RWTH Aachen, Templergraben 55, 52062 Aachen, Germany

A. Krimmel
Hahn-Meitner Institut, Berlin, Germany

G. Nieva
Centro Atomico Bariloche, Bajas Temperaturas, San Carlos de Bariloche, Argentina
(Received 3 December 1996)

The effect of Si doping on the magnetic properties of the spin-Peierls (SP) system $CuGeO_3$ was found to differ strongly between polycrystals (PC's) and single crystals (SC's). In SC's, the SP state is suppressed much more strongly, whereas the existence region of the antiferromagnetic (AF) state is enhanced. We investigated the origin of this difference by means of magnetic susceptibility, specific heat, thermal expansion, Raman scattering, elastic neutron scattering, and x-ray measurements on $CuGe_{1-x}Si_xO_3$ samples prepared under different conditions. The partial oxygen pressure and the temperature during the synthesis were found to have a profound influence on the magnetic properties: preparation under reduced oxygen pressure leads to a stabilization of the AF state, whereas heating above the melting point results in a strong decrease of T_{SP} in Si-doped samples. Therefore, both the AF stabilization and the T_{SP} reduction observed in SC's are not an intrinsic effect of Si doping PC samples, which can be prepared at lower temperatures and more oxidizing conditions, reflect much better the intrinsic properties of $CuGe_{1-x}Si_xO_3$. We were able to prepare PC samples up to 50 at. % Si and found a continuous decrease of the one-dimensional character of the magnetic properties without pronounced changes in the structure. [S0163-1829(97)05321-6]

INTRODUCTION

Since the discovery of $CuGeO_3$ as an inorganic spin-Peierls (SP) system,[1] many investigations have been devoted to this compound (see, for example, Refs. 2–5). The unusual properties of this compound are the consequence of a pronounced one dimensionality of the crystallographic structure:[6] CuO_2 chains along the c axis with a Cu-Cu distance of 2.941 Å are separated from each other by GeO_2 chains, which lead to significantly higher Cu-Cu distances along the a axis (4.81 Å) and the b axis (4.23 Å). Along the Cu chains, short-correlation magnetic fluctuations take place at high temperatures which are coupled to structural fluctuations.[7,8] At $T_{SP}=14.5$ K, a second-order transition into a spin-Peierls state with a crystallographic and magnetic dimerization in the chains and the condensation of the Cu^{2+} spins into a nonmagnetic spin-singlet ground state is observed.

Whereas all other known SP systems are organic materials which are quite unstable against impurities,[9–11] $CuGeO_3$ can easily be doped on both the Ge and the Cu site, offering a possibility of investigating systematically the influence of doping on a SP ground state. Cutting the Cu chains by substituting with Zn leads to a strong reduction of T_{SP} and the suppression of this state at a Zn concentration of ≈ 3 at. %.[2] For higher concentrations, a Néel ground state appears at $T_N=5$ K, which vanishes again with increasing concentration. Similar behavior is observed for other dopands on the Cu site, e.g., Ni, Mn, and Mg.[12] The coexistence range of the SP and the Néel state is generally very small for in-chain dopants.

On the Ge site, only Si doping has been investigated intensively,[13–15] whereas very little is reported on Ti doping.[15] With Si doping, though, strong discrepancies exist between the composition dependence of the magnetic properties observed in single crystals (SC's) and that observed in polycrystals (PC's). T_{SP} is strongly reduced in SC's: the SP state is already suppressed at 2 at. % Si. In contrast, the decrease is very weak in PC's: T_{SP} remains as high as 14.1 K for 10 at. % Si. In addition, the AF state appears at much lower Si concentrations in SC's than in PC's. PC's also indicate that the AF state and the SP state coexist in the doping range 2–4 at. %, whereas this range is much smaller in SC's. Thus, the results on SC's suggest that doping with Si has a much stronger effect on the SP state than doping inside the Cu chains, whereas the results on PC's indicate the exact opposite. Since the effect of impurities on the different crystallographic sites as well as the question of the coexistence of the SP and the Néel state are presently of strong theoretical and experimental interest, it is very important to clarify the intrinsic effect of Si doping and the origin of the observed discrepancy.

EXPERIMENTAL DETAILS

SC's were grown from a $CuGe_{1-x}Si_xO_3$ melt with an excess of 20 wt. % CuO in a Pt crucible by slow cooling at a

rate of 2 °C/h, starting at 1200 °C. The obtained single crystals could easily be separated from the remaining CuO flux; they are transparent blue platelets, cleaving perpendicular to the a axis, with dimensions of (1–2 mm)×(3–6 mm) ×(2–5 mm) along the a, b, and c axis, respectively.

PC's were prepared by a classical powder sintering technique. A stoichiometric mixture of CuO, GeO_2, and SiO_2 was thoroughly mixed, pressed and sintered under ambient pressure at 1000 °C. To increase the homogeneity of the samples, the sintering process was repeated up to three times with intermediate regrindings. To prepare samples under controlled partial oxygen pressure $p(O_2)$, we used a CuO-Cu_2O buffer, similar to the procedure described in Ref. 16: the samples and the buffer are positioned in an evacuated and sealed quartz tube in a way that the sample is kept at 1000 °C, whereas the buffer is kept at a lower temperature. As a consequence, the partial oxygen pressure in the whole tube is controlled by the oxygen pressure of the buffer which is directly a function of the buffer temperature. This is a simple method to control the oxygen pressure during the whole preparation process.

All samples were checked for spurious phases by x-ray diffraction. The lattice constants were determined using Si as an internal standard. Magnetic measurements were carried out in a commercial superconducting quantum interference device magnetometer (MPMS, Quantum Design). The transition temperatures were determined as the crossing point of linear functions fitted above and below the transitions. Raman-scattering experiments were performed with different excitation lines of an Ar Laser using a DILOR-XY spectrometer and a nitrogen-cooled CCD as the detector. Elastic neutron experiments were performed between 2 and 300 K at the Hahn-Meitner Institut and analyzed via Rietveld refinement. Specific-heat measurements were performed using a classical adiabatic technique.[8] Thermal expansion was measured in a capacitance cell described in detail in Ref. 17.

EXPERIMENTAL RESULTS: COMPARISON OF POLYCRYSTALS AND SINGLE CRYSTALS

In PC's, Si doping leads only to a weak suppression of the SP state with a very slight decrease of T_{SP}.[15] The SP transition is seen in susceptibility measurements up to 10 at. % Si (Fig. 1), and the transition temperature remains as high as $T_{SP}=14.1$ K at this Si concentration. At 2 at. % Si doping, the Néel transition appears at $T_N=5$ K, T_N decreasing quite fast to 2.5 K at 4 at. % Si. At higher Si contents, this transition is not visible above 2 K (Fig. 1). Clearly, both transitions coexist for 2–4 at. % Si doping.

This coexistence is also seen in the specific-heat and the thermal-expansion measurements (Fig. 2). At T_{SP}, a sharp transition is observed in both $C_{mag}/T(T)$ and $\alpha(T)$. The size of the anomalies in both measurements is reduced by $\approx 50\%$ in comparison with the undoped compound.[8] The transition at T_N is broadened (due to a somewhat broadened Si distribution (see below) and the strong dependence of T_N on the Si content). Yet, the entropy released at T_N is comparable to the one reported for several in-chain-doped compounds.[18]

The dependence of T_N and T_{SP} on doping we found in our flux grown SC's is very similar to that of SC's grown in an image furnace as reported in the literature.[13] There, in contrast to the PC's samples, a strong suppression of T_{SP} is observed. Already at 1 at. % Si content, the SP transition vanishes completely. The Néel transition appears already at 0.5 at. % Si, the highest value of $T_N=5$ K is obtained at 1 at. % Si, and T_N then decreases slowly with further increasing Si content, being visible in $\chi(T)$ up to more than 6 at. %

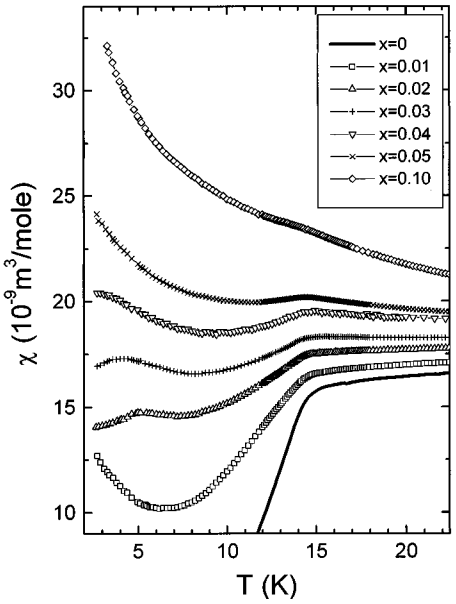

FIG. 1. The susceptibility of $CuGe_{1-x}Si_xO_3$ PC with $x \leqslant 0.1$. The SP transition is seen up to $x=0.1$; T_{SP} remains nearly unchanged. The Néel transition appears at $x=0.02$ ($T_N=5$ K); T_N decreases quite fast with increasing x. Clearly, both phase transitions coexist for $0.02 \leqslant x \leqslant 0.04$.

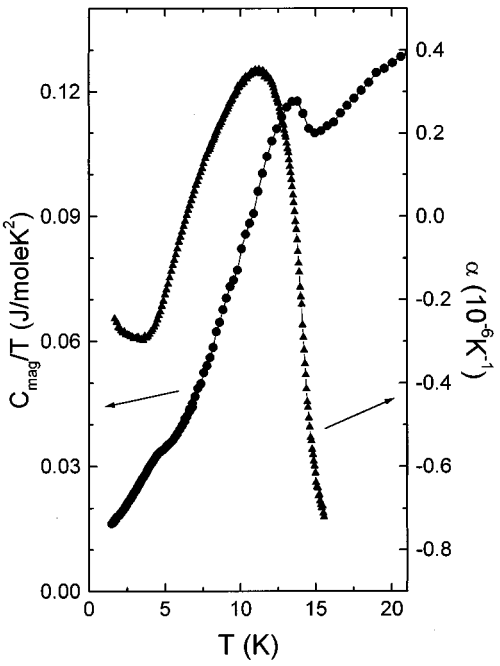

FIG. 2. Specific heat (●) and thermal expansion (s) of a $CuGe_{0.978}Si_{0.022}O_3$ PC. Both measurements were performed on the same sample. Clearly, both measurements prove the macroscopic character of both the SP and the Néel transition.

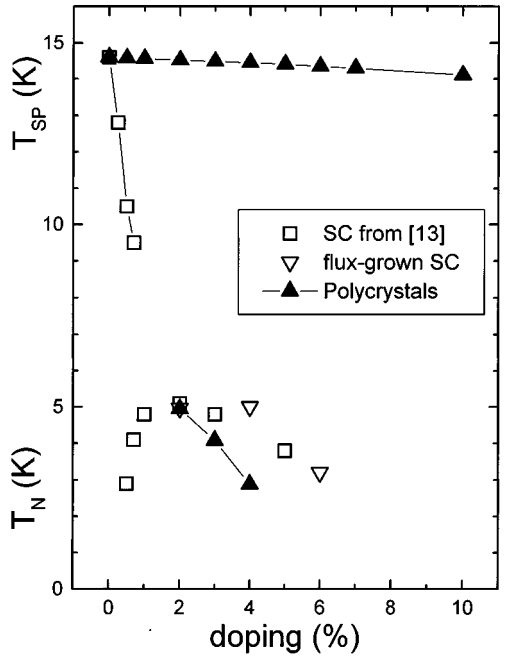

FIG. 3. Comparison of the phase diagram as a function of doping for $CuGe_{1-x}Si_xO_3$ SC's and PC's. SC's reveal the same behavior independent of the growing method, PC's behave strongly different.

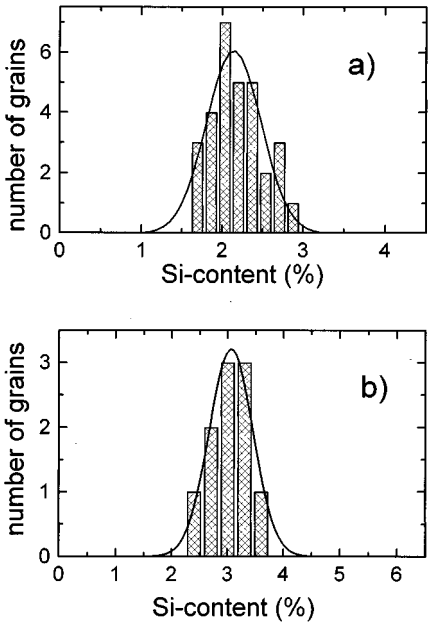

FIG. 4. Histogram of the Si content in single grains of two different PC samples: the $CuGe_{0.978}Si_{0.022}O_3$ PC's (a) used for the specific-heat and thermal-expansion measurements, and a $CuGe_{0.97}Si_{0.03}O_3$ PC (b). The analysis was determined by an EDAX analysis on individual grains of the PC's. The solid line represents a Gauss distribution around the nominal weigh in. Both samples clearly reveal a broadened distribution around the nominal content, but absolutely no indication for a phase separation into an undoped and a higher doped part.

Si. In Fig. 3, we compare the different magnetic phase diagrams of SC's and PC's. Since the magnetic properties of both PC's as well as SC's can be reproduced and seem to be intrinsic to the different types of material, we tried to find the origin of this difference.

To rule out a macroscopic phase separation in PC's in the sense that part of the sample is undoped whereas the remaining part is higher doped than the nominal composition, we performed an energy-dispersive x-ray analysis (EDAX) of individual grains of several PC samples. This analysis revealed a Gauss-like distribution of the Si content with a mean value near the nominal composition (Fig. 4). In the 2.2 at. % Si-doped sample used for the specific-heat and thermal-expansion measurements, the distribution of Si concentrations is broader than in the 3 at. % sample. This difference can be related to the preparation process: only one step was performed for the 2.2 at. % doped sample in order to get a massive block for the specific-heat measurement, whereas the 3 at. % Si-doped sample was homogenized three times leading to a smaller width of the Si distribution. Yet, a macroscopic phase separation into an undoped and an overdoped part can clearly be excluded in both samples. Thus, the magnetic phase diagram observed for PC samples seems to be intrinsic.

We found no difference in x-ray measurements between SC's and PC's; the lattice constants of both depend linearly on the Si content and present the same slope (Fig. 10). Also, Raman experiments showed no significant difference in the phonon spectrum for SC's and PC's (Fig. 11) up to 10 at. % Si (the highest Si concentration investigated in SC's). Yet, the half-widths of the phonons in PC's are about 15 at. % larger than those in SC's probably due to a higher amount of defects in polycrystalline samples in general. So both x-ray as well as Raman measurements reveal no difference in the crystallographic properties of PC's and SC's.

EFFECT OF PREPARATION CONDITIONS ON LOW SI-DOPED SAMPLES

A striking difference between SC's and PC's is the markedly different preparation temperature. As pointed out above, SC's are grown with a starting temperature of $\approx 1200\,^{\circ}C$, which is needed to get a homogeneous melt, whereas PC's are prepared at 1000 °C. Since it is known that compounds containing CuO might be sensitive in this temperature range to a reduction of Cu^{2+} to Cu^{+}, we investigated whether such an effect could influence the properties of $CuGeO_3$.

To perform a first test on the influence of the oxygen content, we prepared a sample with the nominal composition $CuGeO_{2.9}$ partly using Cu_2O instead of CuO as starting material. The sample was sealed in an evacuated quartz tube and heated to 1000 °C. The obtained PC's reveals a strong suppression of the drop in $\chi(T)$ at T_{SP} and a clear Néel transition at $T_N = 4$ K (Fig. 5). This clearly proves that oxygen deficiencies can weaken the SP state and induce the Néel state without the presence of any dopand on the Ge or the Cu site.

In order to investigate the effect of decomposition more systematically, we first performed thermogravity measurements (TGA) and differential thermal analysis (DTA) measurements on pure and Si-doped $CuGeO_3$ at ambient pressure in Al_2O_3 crucibles. Though it is reported that $CuGeO_3$ melts congruently at 1173 °C,[19] we observed already at $T_d = 1100\,^{\circ}C$ a significant loss of mass in TGA (Fig.

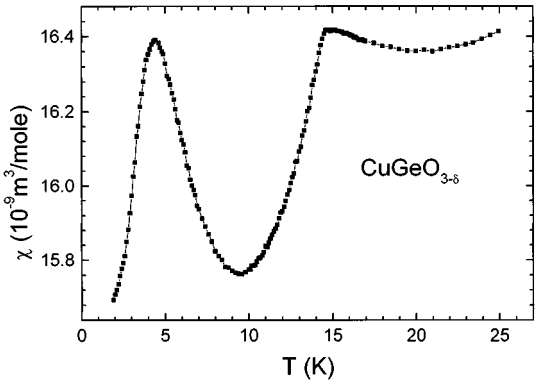

FIG. 5. The susceptibility of an oxygen-reduced undoped PC's $CuGeO_{2.9}$ (see text). The drop in $\chi(T)$ below T_{SP} is strongly suppressed, whereas a pronounced Néel transition is visible at $T_N = 4.2$ K.

6) in conjunction with an endothermic signal in DTA (not shown). This loss of mass can be attributed to the decomposition of $CuGeO_3$ to CuO and GeO_2 along with the reduction of CuO to Cu_2O. After fast cooling of samples heated to 1200 °C, the x-ray analysis of the sample reveals CuO, Cu_2O, and GeO_2 besides $CuGeO_3$. The formation of these decomposition products is already observed when the sample is heated up to 1150 °C, in contrast to what was reported earlier.[19] Thus $CuGeO_3$ presents at ambient pressure some instability starting at a temperature $T_d \approx 1100$ °C, which is significantly above the typical preparation temperature for PC's, but below the growth temperature of SC's. A second peak in the DTA measurements was observed at $T_m \approx 1170$ °C, which we attribute to the melting of the material.

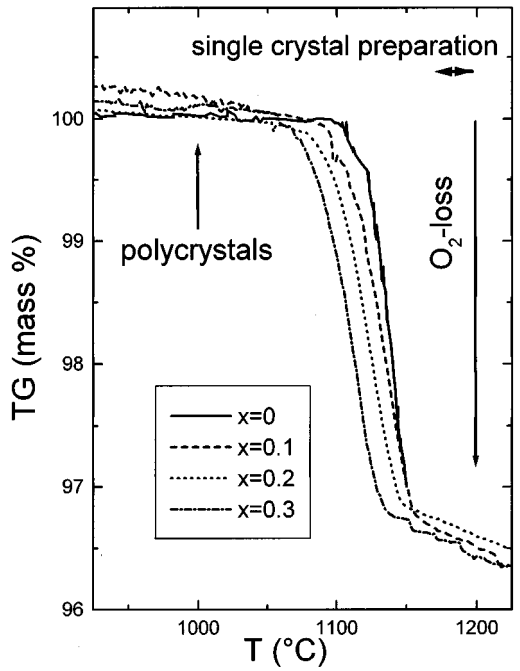

FIG. 6. TGA measurements on $CuGe_{1-x}Si_xO_3$ PC's. The loss of mass is observed at the same temperature where DTA measurements reveal endothermic behavior. The temperature of the onset of this oxygen loss decreases with increasing x. Preparation temperatures of PC's and SC's are indicated.

The TGA and DTA measurements on the Si-doped samples show a systematic reduction of T_d with increasing Si content, indicating a decrease of the stability of $CuGe_{1-x}Si_xO_3$ against reduction (Fig. 6). Extrapolating T_d towards the reduction temperature of CuO at ambient pressure leads to a critical concentration of $x \approx 0.5$, which corresponds to the solubility limit of Si in $CuGeO_3$ (see below). This decrease of the stability of $CuGeO_3$ with increasing Si content is a first hint towards the origin of the corresponding discrepancy between the magnetic properties of PC's and SC's. The melting temperature T_m also shifts to lower temperatures, yet the difference $T_m - T_d \approx 70$ °C remains the same as in the undoped sample.

In order to study the influence of this instability on the magnetic properties, we measured a first set of Si-doped samples prepared at a given temperature, but at different partial oxygen pressure $p(O_2)$ and a second set prepared at ambient pressure, but at different temperatures.

A. Effect of oxygen deficiency

The first set of polycrystalline samples was prepared at 1000 °C under reduced oxygen pressure atmosphere using a CuO-Cu_2O buffer as described above. Except for the oxygen pressure, the preparation of these samples is exactly the same as for unreduced samples.

In an atmosphere with $p(O_2) = 10^{-4}$ bars, the undoped $CuGeO_3$ still forms out of the starting oxides CuO and GeO_2, whereas with 4 at. % Si content, no reaction at all is observed after 60 h. This is an indication that the presence of Si inhibits the formation of $CuGeO_3$.

With $p(O_2) = 10^{-3}$ bars (highly reduced PC's), the samples have a similar optical appearance as the unreduced PC's. Also, no structural differences were observed in x-ray measurements. Nevertheless, the magnetic properties are quite different. Already a doping of 1 at. % Si leads to a Néel transition at $T_N = 4.4$ K. T_N increases to 5.2 and 5.0 K for 2 and 4 at. %, respectively, and is still seen at 2.3 K for 6 at. % Si. Furthermore, though the transition temperature T_{SP} decreases only slightly with respect to unreduced PC's, the decrease of $\chi(T)$ below T_{SP} is much smaller and nearly vanishes at 4 at. % Si (Fig. 7). At higher Si contents, no SP transition was observed. Therefore, highly reduced PC's present exactly the same phase diagram as SC's concerning T_N and a strong suppression of the susceptibility drop at T_{SP} in comparison to unreduced PC's.

PC's prepared at $p(O_2) = 10^{-2}$ bars (weakly reduced PC's) also reveal a phase diagram different from the unreduced PC's. The composition dependence of the anomaly at T_N is the same as in highly reduced PC's and in SC's, whereas no significant difference to unreduced PC's is observed for the behavior at T_{SP}. Again, no change in the crystallographic properties and in the optical appearance with respect to unreduced PC's was observed.

In Fig. 8, we compare the magnetic phase diagram as a function of the Si content for unreduced PC's, highly and weakly reduced PC's as well as SC's. It clearly shows that the T_N vs x dependence in SC's can be reproduced in PC's prepared under reduced oxygen pressure, whereas the T_{SP} vs x dependence is still different between SC's and reduced PC's. However, the similarity between $T_N(x)$ in SC's and

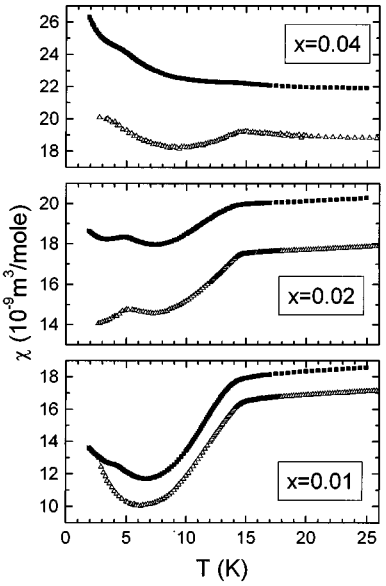

FIG. 7. Comparison of PC's prepared in an atmosphere of 10^{-3} bar O_2 (highly reduced PC's, solid symbols) and at ambient pressure (open symbols). The highly reduced PC's reveal a stabilization of T_N and a suppression of the drop in the susceptibility below T_{SP}; at 4 at. % Si, this drop has nearly disappeared, whereas PC's prepared at ambient pressure still show a clear transition.

reduced PC's already indicates that the behavior of Si-doped SC's do not correspond to the intrinsic properties of stoichiometric Si-doped $CuGeO_3$.

Attempts to reoxidate SC's were not successful. After two annealing steps of 8 h at $T=980$ °C and 180 bars O_2 pressure, T_{SP} was not recovered in a 2.2 at. % Si-doped SC's and T_N remains unchanged. As this might be caused by the low mobility of oxygen in $CuGeO_3$, we crushed the crystal and performed a third annealing step at the same conditions. Yet, the only changes we observed was a small anomaly at $T \approx 14$ K indicating the tendency towards the formation of a SP transition. Also, no change of the lattice constants was observed. These problems of reoxidate SC's within the investigated time scale might be due to an extremely low oxygen mobility within the crystals. Thus, reoxidation of reduced PC's leads to a much stronger shift of their magnetic phase diagram towards the one of unreduced PC's. This larger effect in PC's is probably caused by the high surface/volume ratio and the smaller amount of oxygen defects.

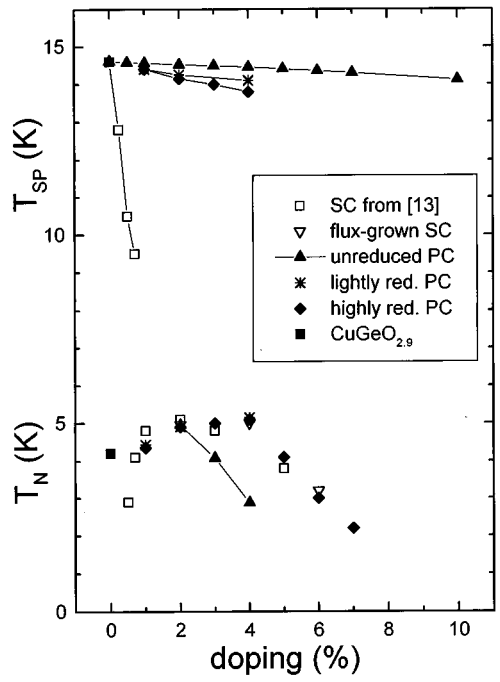

FIG. 8. Comparison of the phase diagram as a function of doping for SC's, reduced PC's and unreduced PC's. Clearly, the behavior of T_N is the same for SC's and reduced PC's, which proves the influence of oxygen deficiency on T_N. T_{SP} is only slightly suppressed for reduced PC's, though the transition vanishes at much lower Si content than for PC's prepared at ambient pressure.

B. Effect of preparation temperature

For the study of the influence of the preparation temperature, a second set of PC samples $CuGe_{1-x}Si_xO_3$ with $0 \leqslant x \leqslant 0.05$ was prepared at ambient pressure at different temperatures between 1050 and 1150 °C. As long as the temperature remains lower than T_m, no significant changes either in the morphology or in the magnetic properties are observed. Once T_m is reached, partial melting of the PC's occurs and leads to the formation of many small single-crystalline grains inside the PC's. Simultaneously, we found a steplike decrease of T_{SP} to the values observed for the SC's.

The sharpness of this change in the magnetic properties is best observed in a 1 at. % Si-doped sample that was prepared at $T_m = 1150$ °C. Due to a small temperature gradient in the furnace, one part of the sample was molten, whereas another part remained polycrystalline. The $\chi(T)$ measurement of the unmolten part still presents a sharp anomaly at $T_{SP} = 14.3$ K, whereas $\chi(T)$ of a piece which was partly molten shows a broad SP anomaly (Fig. 9) starting at $T_{SP}(h) = 14.3$ K (as observed for the PC's of this stoichiometry) and extending down to $T_{SP}(l) = 10.5$ K (corresponding to the value observed for the SC's). Thus this partial melting has an extremely strong effect on the SP state and is clearly responsible for the difference in T_{SP} between PC's and SC's. This strong effect of the melting might be attributed to a different kinematic of the oxygen inside the molten part of the sample.[20] This could, on the one hand, increase the number of oxygen defects, or, on the other hand, cause a different kind of oxygen defect.

For example, the observed stabilization of the Néel phase due to preparation in a reductive atmosphere may be caused by defects on the O(1) site as any disturbance of the lattice is known to stabilize the long-range antiferromagnetic order,[21] whereas in connection with melting a reduction of the O(2)-oxygen content might take place causing an intrinsic doping of the Cu^{2+} chains by reduced Cu^{+}. This would have an effect similar to Zn and could therefore explain the strong decrease of T_{SP} observed in SC's. Also, some Cu holes may occur inside the chains. An occupancy of some Cu sites by Si seems to be unlikely due to the different chemical coordination.[20]

C. Effect of stoichiometry

In addition, we prepared PC's under air at 1000 °C with the stoichiometry $Cu_{1-y}Ge_{1-x}Si_xO_{3-y}$ with $0 \leqslant x \leqslant 0.05$,

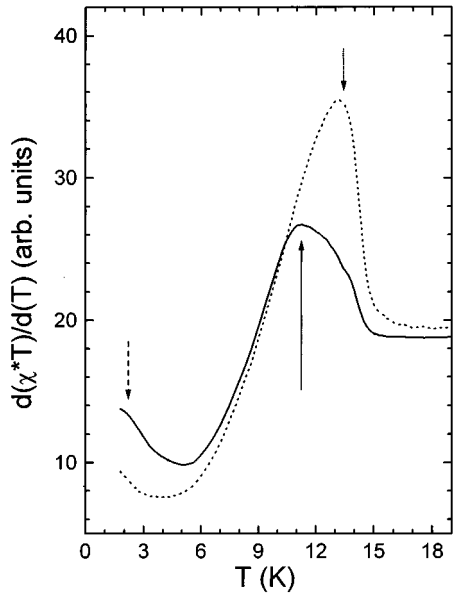

FIG. 9. The susceptibility derivative of two pieces of one $CuGe_{0.99}Si_{0.01}O_3$ PC prepared in a temperature gradient. The piece at the lower temperature remained unmolten, whereas the high-temperature piece was partly molten. $\partial(\chi T)/\partial T$ reveals for the unmolten piece (dotted line) a sharp transition (dotted arrow) at a temperature corresponding to the T_{SP} of PC's. In contrast, the partly molten piece (solid line) reveals a significantly broadened transition starting at the same temperature as the unmolten piece and ending at the temperature corresponding to T_{SP} observed for SC's (solid arrow). In addition, T_N is observed in the partly molten piece (dashed arrow).

$-0.03 \leqslant y \leqslant 0.03$ to check whether an excess or a lack of CuO might also have an influence on the crystallographic and/or the magnetic properties. In all samples with $y \neq 0$, we observed foreign phases: CuO for $y<0$, SiO_2 and GeO_2 for $y>0$, indicating a very narrow homogeneity range for the ratio CuO: (GeO_2,SiO_2). In CuO-deficient samples ($y>0$), we found for $x \geqslant y$ only SiO_2, no GeO_2, as a spurious phase. This indicates a strong preference to incorporate Ge instead of Si: SiO_2 remains unreacted in the amount corresponding to the CuO deficiency.

This preferred incorporation of Ge was also confirmed by the magnetic measurements and the analysis of the lattice constants. In the case of CuO deficiency ($y>0$), samples with a nominal Si content x_{nominal} presents the same magnetic behavior as stoichiometric ($y=0$) samples with a reduced Si content $x_{\text{reduced}}=x_{\text{nominal}}-y$.

For $y>x$, the behavior of an undoped sample ($x=0$) is observed, indicating that no Si was incorporated into the $CuGeO_3$ structure. Samples with an excess of CuO ($y<0$) showed the same magnetic behavior as corresponding stoichiometric samples with the same x and $y=0$.

All the results presented above show that the preparation conditions strongly influence the behavior of $CuGe_{1-x}Si_xO_3$. Preparation at higher temperature and/or reduced oxygen pressure probably lead to a slight oxygen deficiency in the samples. These oxygen deficiencies, on the one hand, stabilize the AF state and enhance its existence range. The differences between SC's and PC's concerning T_{SP}, on the other hand, are clearly related to the different

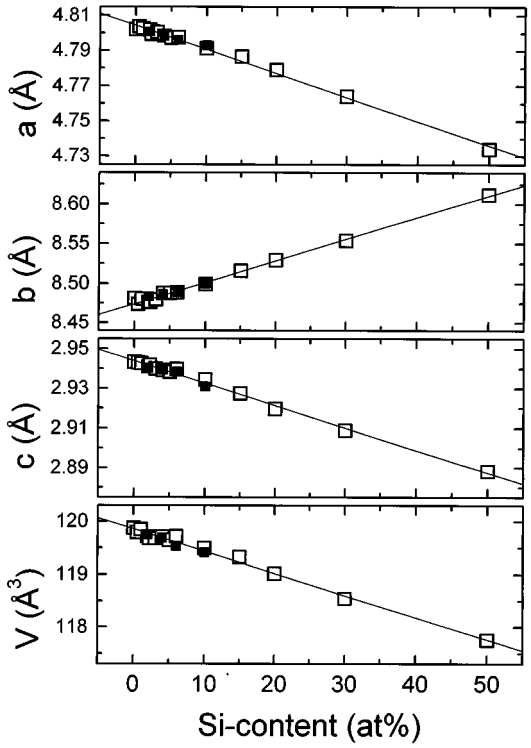

FIG. 10. The lattice constants of $CuGe_{1-x}Si_xO_3$ PC's (□) and SC's (■). Up to the solubility limit of $x=0.5$, all constants and the volume depend linearly on doping. The solid line represents a linear fit to the data. No difference between PC's and SC's is observed.

preparation temperature: the strong suppression of T_{SP} occurs at that very temperature where the samples melt and consequently the kinematic of the preparation is changed. Thus, polycrystalline samples seem up to now to be the only possibility to study the intrinsic effect of Si doping. In the following paragraph, we present further results obtained on Si-doped polycrystalline samples.

PHYSICAL PROPERTIES OF POLYCRYSTALLINE $CuGe_{1-x}Si_xO_3$

We were able to prepare $CuGe_{1-x}Si_xO_3$ with x up to 0.5. The lattice constants depend linearly on the Si content up to the solubility limit with nearly the same slope as it was already reported for small Si content[15] (Fig. 10). The results of the Rietveld refinement of the elastic neutron-scattering experiments for $x=0.05$, 0.1, and 0.3 revealed no change in the crystal structure. Special attention was paid to the O(2) position which determines the Cu-O(2)-Cu angle. This angle plays an important role for the superexchange pathway within the chains. Geertsma and Khomskii,[22] e.g., calculated the decrease of T_{SP} due to Si doping to be caused by a change in the hybridization between the O(2) and the Ge site: the smaller Si ion will attract the O(2) ion, leading to a decrease of the Cu-O(2)-Cu angle towards 90° and consequently a reduction of the antiferromagnetic superexchange. This effect should decrease T_{SP} drastically because each dopant on the Ge site influences two chains.[23] These predictions are in accordance with the strong decrease of T_{SP} observed in SC's, but in contradiction with the small decrease in PC's.

Yet, we found only minor changes in the position of the

TABLE I. Position parameters of the O(2) atom and the Cu-O(2)-Cu angle determined from the elastic neutron measurements on several $CuGe_{1-x}Si_xO_3$ PC at different temperatures. Only very small changes are observed. The data for the undoped sample is taken from Ref. 24.

Si concentration	Temperature	O(2) x	O(2) y	Cu-O(2)-Cu angle
$x=0$	295 K	0.28350	0.08316	99.06°
$x=0$	20 K	0.2816	0.08316	99.24°
$x=0.05$	200 K	0.28402	0.08292	99.18°
$x=0.05$	2 K	0.28075	0.08195	98.96°
$x=0.1$	200 K	0.28766	0.08408	99.51°
$x=0.1$	2 K	0.28485	0.08337	99.33°
$x=0.3$	300 K	0.28629	0.08820	97.89°

O(2) and thus in the Cu-O(2)-Cu angle (Table I). The small effect of Si doping on the Cu-O(2)-Cu angle might explain why the observed decrease of T_{SP} in PC's (see above) due to Si doping is much smaller than was proposed in Ref. 22. In addition, the lattice contraction between room temperature and T_{SP} remains unchanged with respect to the undoped $CuGeO_3$.[23,24] Therefore, all results indicate that the crystal structure remains unaffected by Si doping except for the change in the lattice parameters.

Raman spectroscopy also offers the opportunity to study lattice effects caused by the doping.[25,26] We found a linear shift of the phonon frequency with the doping up to $x=0.3$ (Fig. 11). The relative change is more pronounced than in the lattice constants. The half-width of the phonons increases systematically with increasing Si content. For $x=0.5$, the shift is stronger than the linear extrapolation obtained from lower doping, and the linewidth increases drastically indicating a more drastic change of the dynamical properties and a strongly limited phonon lifetime. In general, all phonons visible at room temperature decrease in intensity with increasing doping level. This loss is typically about 50% for $x=0.3$ compared to the undoped sample $x=0$.

A new phonon as a defect mode is observed at 670 cm^{-1}, growing linearly in intensity as the doping level increases. The frequency ω of this mode can easily be analyzed by using a simple model of an harmonic oscillator with an effective mass m^*

$$\omega \propto \frac{1}{\sqrt{m^*}} \quad \frac{1}{m^*} = \frac{1}{m_{\mathrm{Gel/Si}}} + \frac{1}{m_{\mathrm{O}}},$$

showing the ''original'' mode to be the mixed Ge-O mode at 592 cm^{-1}. Additional defect modes are induced at 203 and 305 cm^{-1}.

Besides, we observe in SC's, where a symmetry analysis is possible, with increasing Si content the appearance of symmetry-forbidden modes, indicating a breaking of the selection rules (Fig. 12). This observation points to a considerable degree of local disorder induced by Si doping.

The results of the susceptibility measurements of low-doped samples were already shown in Fig. 1. With higher Si content, the characteristic signature of the one-dimensional fluctuations gets more and more suppressed: the maximum at

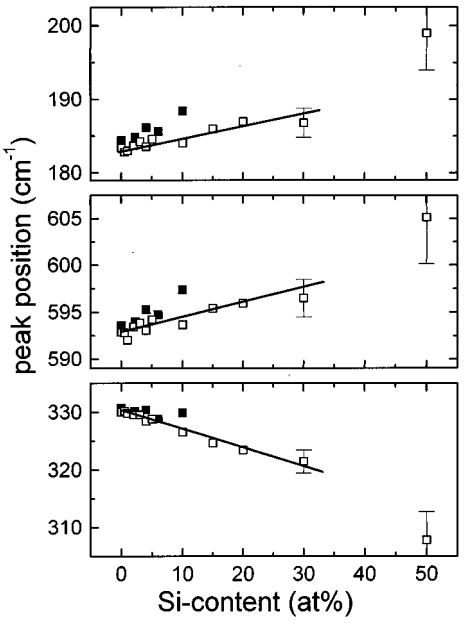

FIG. 11. The optical-phonon frequencies of $CuGe_{1-x}Si_xO_3$ at room temperature. The dependence on the Si content is linear up to $x \leqslant 0.3$. Lines are guides to the eye. The other phonons, which are not shown, remain unchanged. Solid symbols refer to SC's, open ones to PC's. The sample with $x=0.5$ shows a significant larger change of the phonon frequency.

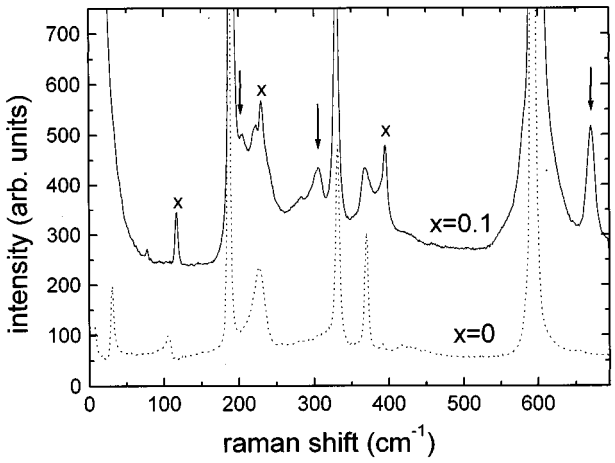

FIG. 12. Normalized Raman-scattering intensity of $CuGe_{1-x}Si_xO_3$ SC's with $x=0$, 0.1. The asterisks mark symmetry-forbidden phonon modes, the arrows defect modes induced by the substitution.

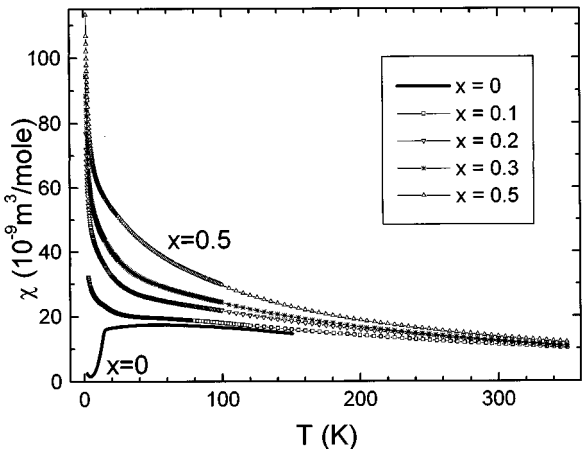

FIG. 13. The susceptibility of $CuGe_{1-x}Si_xO_3$ for $0 \leqslant x \leqslant 0.5$. With increasing Si content, the maximum around $T \approx 56$ K, being characteristic of the one-dimensional behavior, vanishes and is gradually replaced by a Curie-Weiss behavior. For the sake of clarity, only some Si concentrations are shown.

$T_{max} \approx 56$ K disappears with increasing x (Fig. 13). At $x = 0.5$, a Curie-Weiss behavior is observed [Fig. 14(a)] above $T = 50$ K with a Curie constant corresponding to a free Cu^{2+} moment ($\mu = 1.8\mu_B$) and a Curie temperature $\theta = -80$ K, which is approximately the coupling constant in chain direction $J_c \approx 90$ K.[1] In undoped $CuGeO_3$ due to the one-dimensional correlations, the Curie-Weiss law with the same μ and a similar $\theta = -96$ K is only achieved above $T = 400$ K [Fig. 14(b)].

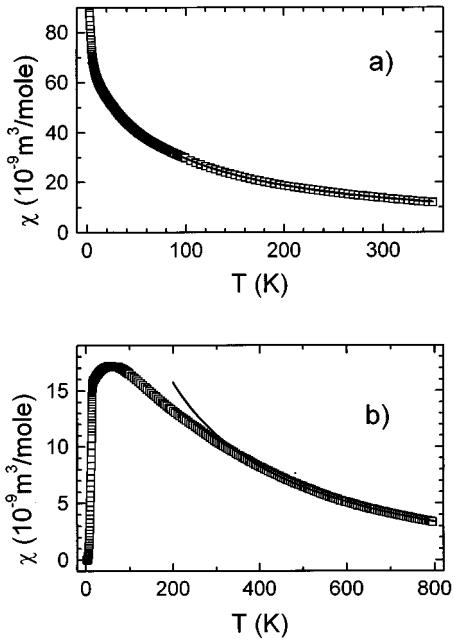

FIG. 14. Curie-Weiss fit for $CuGe_{0.5}Si_{0.5}O_3$ (a) and undoped $CuGeO_3$ (b). The Curie-Weiss behavior is already observed above 50 K in the 50 at. %-doped sample, but only above 400 K in the undoped sample. For both samples, the moment calculated from the Curie constant is $\mu = 1.8\mu_B$, which corresponds to the free Cu^{2+} moment, and the Curie-Weiss temperature is $\theta \approx -80$ K (see text). This corresponds to the strength of the antiferromagnetic exchange along the chains.

Therefore, increasing Si content is more and more shifting the magnetic properties from the one-dimensional behavior to a three-dimensional one. Though, despite the relatively high Curie-Weiss temperature for $x = 0.5$, no long-range magnetic order is observed down to $T = 2$ K. Below 10 K, $\chi(T)$ presents a large increase, which is suppressed with increasing magnetic field, and thus suggests the presence of a spin-glass-like state.

CONCLUSION

Our experiments on Si-doped $CuGeO_3$ showed a profound and reproducible difference between the magnetic phase diagram observed in PC and that observed in SC samples. In PC's, T_{SP} is observed up to 10 at. % Si and decreases only very weakly with increasing Si content. In addition, the SP state coexists with the AF state in a concentration range of 2–4 at. % Si. In constrast, T_{SP} decreases very rapidly in Si-doped SC's, the SP state to be suppressed already below 2 at. % Si, whereas the AF state is observed in a large concentration range.

We clearly showed that these differences are connected with the different preparation conditions, i.e., the synthesis temperature and the oxygen pressure. Preparing PC samples under reduced oxygen pressure leads to a stabilization of the AF state, enlarging its existence region to lower and higher doping contents. Under extremely reductive conditions it is even possible to obtain a well defined AF state in nominally undoped samples.

We further found two critical temperatures T_d and T_m where loss of oxygen and partial melting of the samples, respectively, occurs. Both temperatures decrease with increasing Si content indicating that Si doping results in a decrease of the stability of $CuGeO_3$ against reduction. The melting at T_m of Si-doped PC's results in an abrupt, steplike decrease of T_{SP}. Thus, both the stabilization of the AF state and the decrease of T_{SP} in SC's are clearly correlated to the preparation procedure and are not an intrinsic property of Si doping.

We were able to replace up to 50 at. % Ge by Si in polycrystalline $CuGeO_3$. Besides a strong change of the lattice parameters, no significant structural changes, especially of the Cu-O(2)-Cu angle, were detected. This is supported by Raman scattering. In addition, local disorder induced by Si doping is indicated by broken-symmetry selection rules.

The temperature dependence of the magnetic susceptibility of the highly doped samples indicate a clear decrease of the one-dimensional character without significant decrease of the coupling strength within the chains. However, besides a spin-glass-like signature, no evidence for long-range magnetic order was observed down to 2 K.

ACKNOWLEDGMENTS

This work was supported by SFB 252, SFB 341, and BMBF FKZ.13N6586.

[1] M. Hase, I. Terasaki, and K. Uchinokura, Phys. Rev. Lett. **70**, 3651 (1993).
[2] M. Hase, I. Terasaki, K. Uchinokura, M. Tokunaga, N. Miura, and H. Obara, Phys. Rev. B **48**, 9616 (1993).
[3] K. Hirota, D. E. Cox, J. E. Lorenzo, G. Shirane, J. M. Tranquada, M. Hase, K. Uchinokura, H. Kojima, Y. Shibuya, and I. Tanaka, Phys. Rev. Lett. **73**, 736 (1994).
[4] K. Le Dang, G. Dhalenne, J. P. Renard, A. Revcolevschi, and P. Veillet, Solid State Commun. **91**, 927 (1994).
[5] L. P. Regnault, M. Ain, B. Hennion, G. Dhalenne, and A. Revcolevschi, Phys. Rev. B **53**, 5579 (1996), and references therein.
[6] H. Völlenkle, A. Wittmann, and H. Nowotny, Mh. Chem. **98**, 1352 (1967).
[7] C. H. Chen and S.-W. Cheong, Phys. Rev. B **51**, 6777 (1995).
[8] M. Weiden, J. Köhler, G. Sparn, M. Köppen, M. Lang, C. Geibel, and F. Steglich, Z. Phys. B **98**, 167 (1995).
[9] S. Huizinga, J. Kommandeur, G. A. Sawatzky, B. T. Thole, K. Kopinga, W. J. M. de Jonge, and J. Roos, Phys. Rev. B **19**, 4723 (1979).
[10] S. D. Obertelli, R. H. Friend, D. R. Talham, M. Kurmoo, and P. Day, J. Phys. Condens. Matter **1**, 5671 (1989).
[11] M. Kurmoo, M. A. Green, P. Day, C. Bellitto, G. Staulo, F. L. Pratt, and W. Hayes, Synth. Met. **55–57**, 2380 (1993).
[12] M. Weiden, W. Richter, C. Geibel, and F. Steglich, Czech. J. Phys. **46**, 1973 (1996).
[13] J. P. Renard, K. LeDang, P. Veillet, G. Dhalenne, A. Revcolevschi, and L. P. Regnault, Europhys. Lett. **30**, 475 (1995).
[14] M. Poirier, R. Beaudry, M. Castonguay, M. L. Plumer, G. Quirion, F. S. Ravazi, A. Revcolevschi, and G. Dhalenne, Phys. Rev. B **52**, R6971 (1995).
[15] M. Weiden, W. Richter, C. Geibel, F. Steglich, P. Lemmens, B. Eisener, M. Brinkmann, and G. Güntherodt, Physica B **225**, 177 (1996).
[16] A. Vierling, Ph.D. thesis, T H Darmstadt, 1991.
[17] R. Pott, and R. Schefzyk, J. Phys. E **716**, 445 (1983).
[18] S. B. Oseroff, S.-W. Cheong, B. Aktas, M. F. Hundley, Z. Fisk, and L. W. Rupp, Jr., Phys. Rev. Lett. **74**, 1450 (1995).
[19] E. I. Speranskaya, Inorg. Mater. (Engl. Transl.) **3**, 1271 (1967).
[20] G. Revcolevschi (private communication).
[21] M. Weiden, W. Richter, R. Hauptmann, C. Geibel, and F. Steglich, Physica B (to be published).
[22] W. Geertsma and D. Khomskii, Phys. Rev. B **54**, 3011 (1996).
[23] D. Khomskii, W. Geertsma, and M. Mostovoy, Czech. J. Phys. **46**, 3239 (1996).
[24] M. Braden, G. Wilkendorf, J. Lorenzana, M. Ain, G. McIntyre, M. Behruzi, G. Heger, G. Dhalenne, and A. Revcolevschi, Phys. Rev. B **54**, 1105 (1996).
[25] P. Lemmens, B. Eisener, M. Brinkmann, L. V. Gasparov, G. Güntherodt, P. v. Dongen, M. Weiden, W. Richter, C. Geibel, and F. Steglich, Physica B (to be published); P. Lemmens, M. Udagawa, M. Fischer, G. Güntherodt, P. v. Dongen, M. Weiden, W. Richter, C. Geibel, and F. Steglich, Czech. J. Phys. **46**, Suppl. S4, 1979 (1996); M. Fischer, P. Lemmens, G. Güntherodt, P. v. Dongen, M. Weiden, W. Richter, C. Geibel, and F. Steglich, Physica B (to be published).
[26] H. Winkelmann, E. Gamper, B. Büchner, M. Braden, A. Revcolevschi, and G. Dhalenne, Phys. Rev. B **51**, 12 884 (1995).